

Large Anisotropic Vibrational Correlations in $A15$ Nb_3Ge

G. S. Cargill, III, R. F. Boehme, and W. Weber^(a)

IBM Thomas J. Watson Research Center, Yorktown Heights, New York 10598

(Received 19 January 1983)

Extended x-ray-absorption fine-structure measurements on Nb_3Ge at temperatures from 8 to 300 K using the Nb K edge show large anisotropies in nearest-neighbor vibrational correlations arising from one-dimensional transition-metal chains in the $A15$ structure. A simple view of these vibrations involves combinations of optical phonons which cause chains of Nb atoms to vibrate, nearly undistorted within the bcc lattice of Ge atoms, uncorrelated with vibrations of adjacent, perpendicular Nb chains.

PACS numbers: 63.20.Hp, 74.70.Ps

Nb_3Ge and some other A_3B compounds having the $A15$ (or β - W) structure are of particular interest because of their high-temperature superconductivity and other unusual properties.¹ Much effort has been devoted to investigating the structural, vibrational, and electronic properties of these materials, and especially the interplay of these properties in giving rise to superconductivity. This Letter provides new information from extended x-ray-absorption fine-structure (EXAFS) measurements about the vibrational properties of Nb_3Ge , showing clearly that the anisotropic chain-type ordering of the Nb atoms very strongly affects vibrational correlations between intrachain Nb-Nb neighbors, between interchain Nb-Nb neighbors, and between Nb-Ge neighbors.

EXAFS measurements were made at the Cornell High Energy Synchrotron Source (CHESS) on two different samples of Nb_3Ge , designated sample I and sample II, with the Nb K absorption edge. The polycrystalline samples were obtained by annealing amorphous, sputtered films at 760 K for 24 h.² Microprobe measurements gave compositions 22.5 ± 1 at.% Ge for sample I and 23.2 ± 1 at.% Ge for sample II with less than 0.5 wt.% oxygen. Values of the lattice parameter of the crystallized films were 5.164 ± 0.001 Å for sample I and 5.150 ± 0.002 Å for sample II. Only weak Nb_5Ge_3 lines accompanied the expected Nb_3Ge diffraction lines, and relative peak intensities were similar to those reported by Cox *et al.*,³ for a chemical-vapor-deposited sample of Nb_3Ge . Following Cox *et al.*,³ we estimate that at least 75% of the Nb atoms in our samples occupy A -type sites in the A_3B structure. We measured a T_c onset of 13.5 K for sample I. The fragility and small size of sample II prevented T_c measurements for it. T_c values reported¹ for Nb_3Ge range from about 4 to 21 K. EXAFS measurements were also made on a foil of bcc Nb.

The EXAFS function $\chi(k)$ can be obtained from the absorption coefficient $\mu(E)$ by appropriate background removal and normalization.⁴ In the usual expression for $\chi(k)$,

$$\chi(k) = \sum_j (N_j / k r_j^2) \exp(-2k^2 \sigma_j^2) F_j(k) \times D_j \sin[2k r_j + \varphi_j(k)], \quad (1)$$

$F_j(k)$ is the backscattering amplitude from each of the N_j equivalent neighbors of type j , and $\varphi_j(k)$ is the total phase shift experienced by the photoelectron, including central atom and backscatterer contributions. σ_j^2 is the mean square width of a Gaussian distribution of distances to atoms of type j in a single shell of average radius r_j about the absorbing atom, resulting from thermal vibrations and perhaps static displacements. The scale factor D_j takes approximate account of the photoelectron losses due to inelastic scattering processes. The Fourier transform of $k^2 \chi(k)$ is a radial structure function, $\Phi_2(r)$. Frequently occurring distances r_j produce maxima in $|\Phi_2(r)|$.

The absorption measurements for $A15$ Nb_3Ge and bcc Nb were reduced to obtain $k^2 \chi(k)$ functions, which were Fourier transformed over the interval $k = 3.7$ – 16 Å⁻¹ to obtain radial structure functions $\Phi_2(r)$. Nearly identical results were obtained for the two Nb_3Ge samples. The $|\Phi_2(r)|$ functions are shown in Fig. 1.

Near-neighbor distances and coordination numbers calculated for Nb atoms in bcc Nb ($a_{\text{bcc}} = 3.30$ Å) and in $A15$ Nb_3Ge ($a_{A15} = 5.16$ Å) are listed in Table I. In $|\Phi_2(r)|$ the maxima are shifted from these values to smaller distances by about 0.35 Å because of the $\varphi_j(k)$ phase shift in Eq. (1). The first three near-neighbor shells for Nb_3Ge are contained within the split maximum between 1.5 and 3.5 Å of $|\Phi_2(r)|$ shown in Figs. 1(b) and 1(c).

As expected, the amplitudes of $\chi(k)$ and $\Phi(r)$

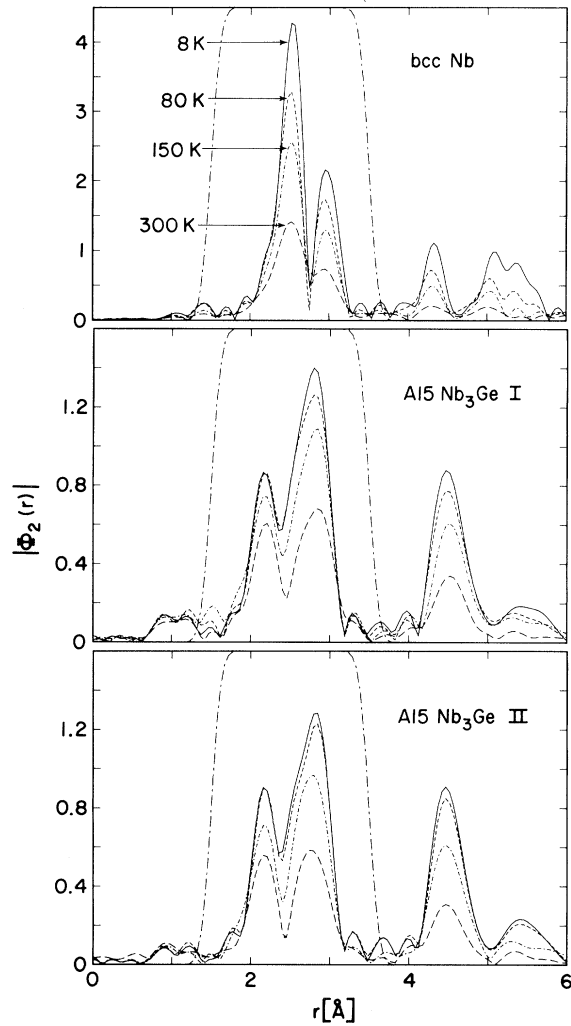


FIG. 1. $|\Phi_2(r)|$ radial structure functions for bcc Nb and for two samples of A15 Nb₃Ge from EXAFS measurements at 8, 80, 150, and 300 K. Also shown are the window functions used in back-transforming the near-neighbor regions, as discussed in the text. The maxima in $|\Phi_2(r)|$ are shifted from values given in Table I because of the $\varphi_j(k)$ phase shift in Eq. (1).

for both bcc Nb and A15 Nb₃Ge are reduced as the measurement temperature is increased. The reductions arise, in the simplest case, from increase with temperature of σ_j^2 in the Debye-Waller term in Eq. (1). With increasing temperature, the two prominent maxima in $|\Phi_2(r)|$ for bcc Nb decrease in height at about the same rate; however, in A15 Nb₃Ge the intrachain Nb-Nb maximum is much more persistent than the interchain Nb-Nb maximum or the composite maximum between 4 and 5 Å.

The temperature dependence of σ_j^2 for the various near-neighbor pairs in A15 Nb₃Ge and in bcc

TABLE I. Near-neighbor distances and coordination numbers for Nb atoms in bcc Nb and A15 Nb₃Ge for $r < 4$ Å.

j	bcc Nb		A15 Nb ₃ Ge		Type
	r_j (Å)	N_j	r_j (Å)	N_j	
1	2.86	8	2.58	2	Nb-Nb intrachain
2	3.30	6	2.88	4	Nb-Ge
3			3.16	8	Nb-Nb interchain

Nb were obtained by fitting near-neighbor model $k^2\chi(k)$ functions, over the range $k = 5-15$ Å⁻¹, to the corresponding experimental functions obtained by back-transforming the near-neighbor regions of the $\Phi_2(r)$ by use of the window functions shown in Fig. 1. Calculated phase shifts and backscattering amplitudes⁵ and the measured monochromator resolution were used in the model calculations.

Fits were first made at each temperature to the bcc Nb data, with use of two neighbor shells, and varying one scale factor $D_{\text{bcc-Nb}} = D_1 = D_2$, one mean square width $\sigma_{\text{bcc-Nb}} = \sigma_1^2 = \sigma_2^2$, and a shift in the zero of the energy scale⁵ ΔE_0 . The scale factors for each of the temperatures were nearly the same, $D_{\text{bcc-Nb}} = 0.70 \pm 0.02$, and $\sigma_{\text{bcc-Nb}}$ increased with increasing temperature as shown in Fig. 2.

Fits were then made to the Nb₃Ge data, with use of three neighbor shells, fixing the three scale factors to be 0.70 as determined for bcc Nb, and varying the three mean square widths σ_j^2 and the zero shift ΔE_0 . The resulting values of $\Delta\sigma_j^2(T) = \sigma_j^2(T) - \sigma_j^2(8\text{ K})$ are shown in Fig. 2.

The EXAFS Debye-Waller factor $\exp(-2k^2\sigma_j^2)$, its limits of validity, and its relation to the x-ray-scattering Debye-Waller factor $\exp(-q^2 \times \langle u_{\vec{q},j}^2 \rangle)$ have been discussed elsewhere.⁶⁻⁸ In the EXAFS case, σ_j^2 is the mean square fluctuation about r_j of the interatomic distance between the absorbing atom and its j th neighbor, and it therefore involves *relative* displacements. However, $\langle u_{\vec{q},j}^2 \rangle$ is the mean square *absolute* displacement, parallel to the scattering vector \vec{q} , for atoms of type j from their equilibrium lattice sites. A temperature-dependent correlation or coupling function γ_j connects relative displacements σ_j^2 and absolute displacements $\langle u_{\vec{q},j}^2 \rangle$.

For a cubic, monatomic material the relationship between the two types of displacements is simply $\sigma_j^2 = 2\gamma_j \langle u^2 \rangle$. In this case, $\langle u^2 \rangle$ is isotropic, and γ_j is the same for all atoms within a

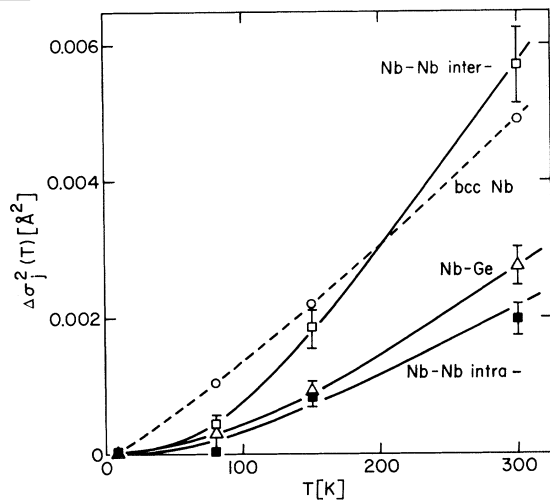


FIG. 2. Temperature dependence of $\Delta\sigma_j^2(T) = \sigma_j^2(T) - \sigma_j^2(8\text{ K})$ for bcc Nb shown with circles, and for A15 Nb_3Ge shown with filled squares for Nb-Nb intrachain pairs, open squares for Nb-Nb interchain pairs, and triangles for Nb-Ge pairs. Values plotted for Nb_3Ge are averages for samples I and II, and vertical bars extend to individual values for these samples. Lines are drawn simply connecting data points.

given coordination shell. For uncorrelated displacements, as expected for distant neighbors and high temperatures, $\gamma_j = 1$, but for correlated displacements, $\gamma_j \neq 1$.

For an A_3B A15 compound, $\langle u_{\parallel}^2 \rangle$ is isotropic for B site but is a two-component tensor for the A site: $\langle u_{\parallel}^2 \rangle$ and $\langle u_{\perp}^2 \rangle$. Likewise, γ_j and σ_j^2 are expected to be different for Nb-Nb intrachain nearest neighbors, for Nb-Nb interchain nearest neighbors, and for Nb-Ge nearest neighbors.

We cannot give a definite interpretation for individual values of $\sigma^2(T)$ obtained from fitting our EXAFS measurements. These values can be affected by errors in the shape of calculated $F_j(k)$ functions and by k dependence of inelastic loss processes, as well as by true distributions of the near-neighbor distances, either static or thermal in origin. Interpretation of $\Delta\sigma_j^2(T) = \sigma_j^2(T) - \sigma_j^2(8\text{ K})$ as the increase in mean square thermal fluctuation in distance r_j for temperature increases from 8 K involves fewer uncertainties, since the nonvibrational factors are expected to be temperature independent. As shown in Fig. 2, $\Delta\sigma^2(T)$ data for the different types of nearest neighbors in Nb_3Ge have very different temperature dependences and magnitudes. Differences between intrachain and interchain Nb-Nb values of $\Delta\sigma^2(300\text{ K})$, i.e., anisotropy in the distance

fluctuations,

$$(\Delta\sigma_{\text{inter}}^2 - \Delta\sigma_{\text{intra}}^2) / \Delta\sigma_{\text{inter}}^2 = 0.66, \quad (2)$$

are much larger than anisotropies reported⁹ in Bragg x-ray-scattering Debye-Waller factors $\langle u^2 \rangle$ for A15 compounds: 0.355 for Nb_3Al , 0.208 for V_3Si , and 0.121 for Cr_3Si . No anisotropic $\langle u^2 \rangle$ values have been reported from scattering measurements on Nb_3Ge .

The large differences between $\Delta\sigma_{\text{Nb-Nb inter}}^2(T)$ and $\Delta\sigma_{\text{Nb-Nb intra}}^2(T)$ could arise, in principle, either from anisotropy in the mean square vibrations of Nb atoms with respect to their equilibrium lattice sites $\langle u^2 \rangle$ or from anisotropy in the vibrational coupling function $\gamma(r)$. Since the observed anisotropy in $\Delta\sigma_{\text{Nb-Nb}}^2$ is much larger than anisotropies in $\langle u^2 \rangle$ for other A15 compounds (Nb_3Al , V_3Si , Cr_3Si),⁹ the anisotropy in $\Delta\sigma_{\text{Nb-Nb}}^2$ for Nb_3Ge probably reflects a large anisotropy in the vibrational coupling factor γ_j , i.e., Nb-Nb intrachain nearest-neighbor atoms tend to vibrate in phase to a much greater degree than do Nb-Nb interchain nearest neighbors. A very simple view of these vibrations involves combinations of optical phonons which cause chains of Nb atoms to vibrate, nearly undistorted within the bcc lattice of Ge atoms, uncorrelated with vibrations of adjacent, perpendicular Nb chains. These types of optical modes would be inaccessible by ultrasonic measurements. Our values of $\Delta\sigma_{\text{Nb-Ge}}^2(T)$ are less reliable than those for Nb-Nb, since the Nb-Ge contribution is weaker and is not resolved as a separate maximum in $|\Phi_2(r)|$. Our value of $\sigma_{\text{Nb-Ge}}^2(300\text{ K}) - \sigma_{\text{Nb-Ge}}^2(80\text{ K})$ is 40% smaller than that reported by Claeson, Boyce, and Geballe,¹⁰ from Ge *K*-edge EXAFS, but our value of $\sigma_{\text{Nb-Nb inter}}^2(300\text{ K}) - \sigma_{\text{Nb-Nb inter}}^2(80\text{ K})$ is the same as their value for Ge-Nb second and fourth shell neighbors.

Although the information provided by our EXAFS measurements, $\Delta\sigma_j^2(T)$, could be calculated from an accurate lattice-dynamics model for the A15 compound,⁶⁻⁸ it seems unlikely that such a model can be developed without extensive inelastic neutron-scattering measurements requiring single-crystal samples. In the absence of a systematic understanding of lattice dynamics in A15 Nb_3Ge , the EXAFS results illuminate a new aspect of atomic vibrations which may play a role in A15 superconductivity.

We gratefully acknowledge materials and advice provided by C. C. Tsuei, microprobe analysis provided by F. Cardone and R. J. Savoy, programming done by A. A. Levi, and assistance

with the EXAFS measurements provided by the staff of CHESS.

^(a)Present address: Sektion Physik der Ludwig-Maximilians Universität München, 8000 München 22, West Germany.

¹L. R. Testardi, in *Physical Acoustics*, edited by W. P. Mason and R. N. Thurston (Academic, New York, 1977), Vol. 13, p. 29.

²R. A. Pollak, C. C. Tsuei, and R. W. Johnson, *Solid State Commun.* **23**, 879 (1977).

³See Fig. 1 (unirradiated) in D. E. Cox, A. R. Sweedler, S. Moehlecke, L. R. Newkirk, and F. A. Valencia, in *Superconductivity in d- and f-band Metals*, edited by

H. Suhl and M. B. Maple (Academic, New York, 1980), p. 335.

⁴See, for example, P. A. Lee, P. H. Citrin, P. Eisenberger, and B. M. Kincaid, *Rev. Mod. Phys.* **53**, 769 (1981).

⁵B. K. Teo and P. A. Lee, *J. Am. Chem. Soc.* **101**, 2815 (1979).

⁶G. Beni and P. M. Platzman, *Phys. Rev. B* **14**, 1514 (1976).

⁷E. Sevallano, H. Meuth, and J. J. Rehr, *Phys. Rev. B* **20**, 4908 (1979).

⁸W. Böhmer and P. Rabe, *J. Phys. C* **12**, 2465 (1979).

⁹R. Flükiger, J. L. Staudenmann, and P. Fischer, *J. Less-Common Met.* **50**, 253 (1976).

¹⁰T. Claeson, J. B. Boyce, and T. H. Geballe, *Phys. Rev. B* **25**, 6666 (1982).